

# Evaluation on the Cooling Capacity of a Cascade Cold Storage Refrigeration System Using Refrigerant Pair R513A/R744

Vinhngi Le<sup>1</sup>, Thanhtrung Dang<sup>1,\*</sup>, Huuquyen Nguyen<sup>1</sup>, Hay Nguyen<sup>1</sup>,  
Hoangtuan Nguyen<sup>1</sup>

<sup>1</sup>Department of Thermal Engineering, Ho Chi Minh city University of Technology and Engineering, Ho Chi Minh city 71307, Viet Nam

\*Author to whom correspondence should be addressed:  
E-mail: trungdang@hcmute.edu.vn

(Received June 09, 2025; Revised August 24, 2025; Accepted August 25, 2025)

**Abstract:** This paper presented in a cascade cold storage refrigeration system using a R513A/R744 pair by the experimental method. The R744 refrigerant was used for the low temperature cycle (LTC) and R513A was used for the high temperature cycle (HTC). The experimental data on the thermodynamic properties were collected at an ambient temperature of 32°C. Following this study, the thermal parameters of those refrigerants in CRS were indicated detailly, the temperature of cold room was gone from 32°C down to -20°C in 35 minutes. The R744 refrigerant in LTC has a condensing temperature of 5.9°C and an evaporating temperature of -25°C, experimenting with the cooling capacity reached 1.35 kW and the overall COP reached 2.0. Moreover, those theory results are suitable with experimental data, the differential error is less than 10%.

**Keywords:** cascade; cold storage; cooling capacity; R513A/R744; refrigerant

## 1. Introduction

Nowadays, refrigeration systems using HCFCs (HydroChloro FluoroCarbons) and HFCs (HydroFluoroCarbons) refrigerants cause a greenhouse effect and the impact of penetrating the Earth's ozone layer, thereby changing the global climate. Therefore, some refrigerants that have little impact on climate change and environmental protection have been selected to replace chlorine atom-containing fluids in some refrigeration systems.

Regarding the studies on low GWP (Global Warming Potential) refrigerants to protect the environment in the heating and cooling cycles, Purjam et al. studied the refrigeration cycle of the R744 ejector operating transcritical and supercritical at fixed pressures that affect COP (Coefficient of Performance)<sup>1</sup>. Reaching supercritical conditions for the ejector's thrust pressure, the combined expansion rate increases the system efficiency. Sachdeva et al. studied the ejector refrigeration system with low GWP R1234ze and R134a using the Gouy-Stodola formula to determine the maximum COP<sup>2</sup>. Widianti and Firdaus used Biblioshiny software to analyze an overview of studies on the Organic Rankine Cycle (ORC) on various fluids including R744, R290, and HFOs (HydroFluoroOlefins) such as R1234yf, R1234ze, and R152a<sup>3</sup>. Kibria et al. investigated the indirect emission and

the warming impact of some refrigerants with the different locations in Japan<sup>4</sup>). Ashwni et al. studied the exergetic and COP of the zeotropic mixtures of the pairs include R245fa/R152a, R600/R152a, and R245fa/R600 in both ORC cycle and VCR cycle<sup>5</sup>). Replacing R410A for domestic heat pumps, Yang et al. studied on Low-GWP refrigerant blends<sup>6</sup>). However, studies<sup>1-6</sup>) did not experiment with a cascade refrigeration system (CRS) using refrigerant pair R513A/R744.

Regarding the refrigeration cycle operating transcritical, recent studies have come up with different system configurations to achieve the highest COP. Amaris et al. conducted a comparative study of three systems: the R744 high pressure cycle, the R744 high pressure cycle with a parallel compressor, and the R717/R744 CRS for food retail applications to investigate performance based on Thermodynamic Laws I and II<sup>7</sup>). Nebot-Andres et al. determined in experiment to optimize operation conditions of the R744 transcritical refrigeration system for the integration of the subcooling mechanism<sup>8</sup>). The system was tested under various pressure and cooling conditions to obtain optimal COP under ambient temperatures of 25°C, 30.4°C, 35.1°C while the evaporation temperature from -15.6°C to -4.1°C. Goodarzi and Gheibi analyzed the efficiency of a 2-stage cycle with an internal heat exchanger (IHE), intermediate cooler, ejector, and liquid

separator using R744<sup>9</sup>). The new cycle under the same operating conditions improved COP by up to 26.9% compared to the original cycle. Chen et al. experimentally investigated the transcritical R744 refrigeration system for cars, using dual rotors and an intercooler for compressors<sup>10</sup>). At an ambient temperature of 45°C, the system efficiency has a 19.8% higher cooling capacity and a corresponding increase of 12.8% in COP to the basic cycle. Manjili and Cheraghi used EES (Engineering Equation Solver) software to analyze the thermodynamics and exergetics of the R744 refrigeration cycle on a 2-stage transcritical using 2 ejectors, each vapour compression line consisting of a separate ejector<sup>11</sup>). COP system was improved by 20% - 80% compared to the conventional cycle. The efficiency of IHE in the transcritical R744 refrigeration cycle using ejectors was theoretically evaluated by Zhang et al.<sup>12</sup>). Under the same cooling pressure condition, the ejector efficiency increases and the static pressure decreases.

In addition, there have been quite a lot of studies related to the subcritical operating refrigeration systems studied. Silva et al. compared the energy and cooling efficiencies of three refrigeration systems: R744/R404A and two direct expansion refrigeration systems R404A and R22<sup>13</sup>). Zhang et al. experimented with the performance of the R1270/R744 compressor that specifically designed for the R1270 (cannot be found in the market) to compare it with the conventional R1270/R744<sup>14</sup>). The results show that the COP of CRS increases by decreasing the  $T_{Evap}$  of R1270 from  $-7^{\circ}\text{C}$  to  $-19^{\circ}\text{C}$ . The effects of climate on R1234ze/R744 with a solar-powered ejector were analyzed by Li et al.<sup>15</sup>). The results show that with the increase in  $T_{Evap}$  R1234ze, the injection ratio and the cooling capacity increase. Decreasing the temperature different  $\Delta t$ , the COP decreases. Lizarte et al. studied an ORC combined with a CRS using natural refrigerants<sup>16</sup>). Dokandari et al. evaluated the performance of the R744/R717 with the new expansion ejector by studying the impact of three design parameters,  $T_{Cond}$ ,  $T_{Evap}$ , and temperature differential at the heat exchanger<sup>17</sup>). The results show that the maximum COP and the maximum Thermodynamic Law II efficiency are 7% and 5% higher on average respectively. Megdouli et al. analyzed the thermodynamics of R744/NO<sub>2</sub> with a new extended ejector for low-temperature refrigeration applications<sup>18</sup>). Sobieraj and Rosinski experimentally studied the R744/R600a high-efficiency phase separation for low-temperature isothermal refrigeration systems<sup>19</sup>). The results show that the system was very sensitive to refrigerant charging. The system does not work accurately due to the cut-off point of the heat exchanger with the low refrigerant quantity. The higher the refrigerant quantity, the higher the power consumption leading to the decrease of COP. Aminyavari et al. successfully analyzed the exergetic performance, economics, environmental properties, and optimization of R744/R717. Optimal

design parameters (exergetic efficiency and total cost ratio) were achieved by using genetic algorithm and then using the TOPSIS decision-making method<sup>20</sup>). Ma et al. fulfilled a performance evaluation and analysis of the optimal configuration of R744/R717 CRS with a Membrane Condensation – Evaporation unit<sup>21</sup>). The results show an improvement in the COP by the small temperature difference of the cascade heat exchanger (CHE). Moreover, Logesh et al. successfully analyzed the performance of a CRS with three different pairs of refrigerants: R134a/R23, R410A/R23, R404A/R170 in the superheat temperature of 10°C and the subcooling of 5°C<sup>22</sup>). The results showed that the R134a/R170 pair had a higher COP and lower flow rate in the study pairs. Next, Gautam et al. conducted a subcritical to supercritical analytical study for evaporators with temperatures ranging from  $-5^{\circ}\text{C}$  to  $15^{\circ}\text{C}$ <sup>23</sup>) to achieve the maximum COP and the maximum specific cooling efficiency. Regarding the R744/R32 water heat pump system, Sun et al. evaluated its performance both cooling and heating in a varying compressor operating condition<sup>24</sup>). Heating efficiency ( $\text{COP}_h$ ) and cooling efficiency ( $\text{COP}_c$ ) results improved by up to 23.3% and 65.2% in heating capacity, cooling capacity, respectively.

Regarding the comparison of the performance of the CRS compared to HFC two-stage refrigeration system (TSRS), Messineo conducted an evaluation of the performance of the R744/R717 CRS compared to the HFC TSRS in terms of energy, safety and environment<sup>25</sup>). The results show that the CRS is a good replacement to the R404A TSRS for low evaporation temperatures (from  $-30^{\circ}\text{C}$  to  $-50^{\circ}\text{C}$ ) in commercial refrigeration. Ghosh et al. optimized system COP and energy efficiency in a R744/R1234yf CRS with focusing evaporation temperature and condensation temperature<sup>26</sup>). Ustaoglu et al. used ANOVA approaches and Taguchi method to find the maximum COP and exergetic efficiency optimization in a CRS using R744 at LTC and R404A, R134a, R510A at HTC<sup>27</sup>). Liu et al. analyzed the thermodynamics of the transcritical R744 refrigeration cycle with an integrated thermoelectric subcooler and ejector to compare it with two independent transcritical R744 cycles: (1) with the thermoelectric subcooler and (2) with the ejector<sup>28</sup>). The results indicate the maximum cooling efficiency of the performance achieved for the integrated cycle with the same optimization of the cold temperature and discharge pressure. Dang et al. numerically simulated the evaporator and the condenser of R744 air conditioning systems; however, a CRS using R744 was not mentioned in the studies<sup>29,30</sup>).

Related to the application potential studies of R513A, Yang et al. compared the characteristics between R134a and R513A, mainly in residential refrigerators in experiment<sup>31</sup>). Three types of tests were performed under the same environmental conditions. It indicated that the optimal gas charging for R513A is 5.9% lower than that of

R134a. R513A is quite superior in residential refrigeration applications. Babiloni et al.<sup>32-34</sup> experimentally analyzed between R134a and R513A<sup>32-34</sup> with the evaporation temperature ranges from -15°C to 5°C. The results show that the highest exergy destruction at the compressor. The discharge temperature of R513A compressor is lower than the R134a. Sun et al. examined some parameters including cooling capacity, COP, and exergy performance between the R513A and R134a systems<sup>35</sup>. The power consumption of R513A system is reduced by up to 12% under most operating conditions.

Through the above studies, the thermodynamic behaviors for the R513A/R744 cascade cold storage refrigeration system have not been studied much; therefore, it is important to conduct reasonable research. Following this study, the system cooling capacity was about 1.5 kW, the evaporation temperature of the R744 medium was -25°C, and the cold room temperature was -20°C. Experimental data of the R513A/R744 pair was compared to the R134a/R744 pair under the same experimental conditions.

## 2. Methodology

### 2.1. Governing equations

To analyze and evaluate the R513A/R744 CRS through the COP system, the governing equations for the entire system include the LTC and the HTC are determined as below:

- LTC with R744 refrigerant

The system cooling capacity is:

$$Q_{0(R744)} = m_1 \times (h_1 - h_4) \quad (1)$$

The R744 mass flow rate was calculated as:

$$m_1 = \frac{Q_{0(R744)}}{h_1 - h_4} \quad (2)$$

where  $h$  is enthalpy (kJ/kg)

The isotropic power input was calculated by:

$$N_{(R744)} = m_1 \times (h_2 - h_1) \quad (3)$$

The IHE capacity was calculated as:

$$Q_{K(R744)} = m_1 \times (h_2 - h_3) \quad (4)$$

The COP for the R744 cycle was determined by:

$$COP_{R744} = \frac{Q_{0(R744)}}{N_{(R744)}} \quad (5)$$

where  $N$  is the isotropic power (W)

- HTC with R513A refrigerant

The cooling capacity for R513A side was determined by:

$$Q_{0(R513A)} = Q_{K(R744)} \quad (6)$$

The R513A mass flow rate was calculated as:

$$m_2 = \frac{Q_{0(R513A)}}{h_1 - h_4} \quad (7)$$

The R513A isotropic power input was calculated by:

$$N_{(R513A)} = m_2 \times (h_2 - h_1) \quad (8)$$

The R513A condenser capacity was calculated as:

$$Q_{K(R513A)} = m_2 \times (h_2 - h_3) \quad (9)$$

The COP of the R513A cycle was determined by:

$$COP_{R513A} = \frac{Q_{0(R513A)}}{N_{(R513A)}} \quad (10)$$

The system COP was calculated by:

$$COP = \frac{Q_{0(R744)}}{N_{(R744)} + N_{(R513A)}} \quad (11)$$

### 2.2. Experimental set up

The experimental diagram of cascade system for R513A/R744 was indicated on Figure 1. Following this study, the R513A was used for HTC and the R744 was used for LTC, it was operated to collect thermodynamic parameters such as temperature, pressure of both R513A and R744. Also, the evaporating temperature of R513A is transposed from 0.8 to 20°C and the evaporation temperature of R744 is kept at -25°C. A welding plate heat exchanger was used for the CHE (Figure 2). Also, the time for reaching the temperature of cold room (from 32°C to -20°C) is approximately 35 minutes.

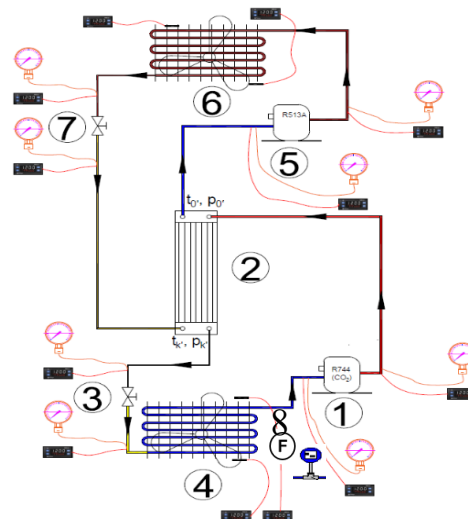


**Fig. 1:** The principal diagram and position of measuring device in the R513A/R744 cascade system (1 – R744 Compressor, 2 – CHE (welding plate), 3 – R744 Expansion valve, 4 – R744 Evaporator, 5 – R513A Compressor, 6 – R513A Condenser, 7 – R513A Expansion valve, 8 – Thermal flow meter).



Fig. 2: Photos of R513A/R744 cascade system

Table 1: Information on the measuring apparatuses

Measuring device	Accuracy	Range
Thermocouples	± 0.1 °C	0-100 °C
Amp-clamp	± 1.5 % rdg	0-200 A
Anemometer	± 3 %	0-45 m/s
Pressure gauge	± 1 FS	0-100 kgf/cm <sup>2</sup>
Pressure sensor	± 0.5 FS	0-100 bar
Turbine flow meter	± 0.5 RS	400-5000 l/h

The accuracy specifications and testing ranges of apparatuses are indicated in Table 1. The experimental devices consist of thermocouples, amp-clamp, anemometer, pressure sensor, pressure gauge, turbine flow meter, etc. The anemometer was used to measure the air velocity for determining the cooling capacity.

### 3. Results and Discussion

The system was experimented many times to gather the operational data in the surroundings temperature around 32°C. The volumetric flow of the R744 was collected by a turbine flow meter with a merit of 270l/h. The results of the R744 test in LTC are shown in Table 2. A cycle superheat of 18.5°C can be observed. Based on experimental data, the thermodynamic point of the LTC is displayed in Figure 3 which was drawn in the EES software.

Table 2: The experimental data for R744 in LTC

Points	t (°C)	p (bar)	h (kJ/kg)
1	-26	16.75	437.06
1'	-6.5	16.75	433.89
2	62	36.65	501.65
3	5.8	36.65	215.08
3'	3.4	36.65	208.82
4	-26	16.75	208.82

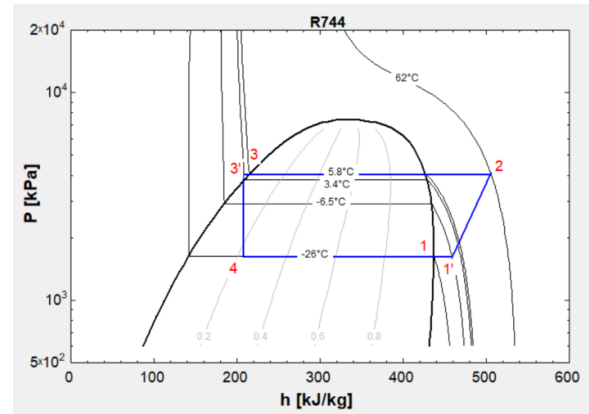


Fig. 3: p-h of R744 in the LTC

Table 3: The experimental data for R513A in HTC

Points	t (°C)	p (bar)	h (kJ/kg)
1	0.8	2.5	399.19
1'	5	2.5	401.49
2	58.2	9.8	426.07
3	34.7	9.8	247.6
3'	30.6	9.8	241.72
4	3	2.5	241.72

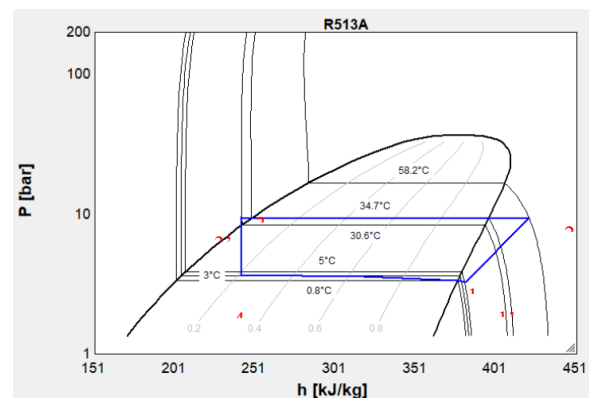


Fig. 4: p-h of R513A in HTC

With the high temperature cycle of R513A, the experimental data are displayed in Table 3 and Figure 4. The temperature variation in the CHE is about 3°C. The results of R513A and R744 showed that at a saturation pressure, the testing temperature has a difference with the theoretical calculation; the difference is due to experimental inaccuracy. However, the experimental data are in quite conformity with those gained from calculation and the inaccuracy is less than 10%.

The experimental data was studied on the evaporating temperature in a cycle of R513A was changed from 0.8 to 4.3°C and the stable evaporating temperature with R744 is -25°C in the LTC. Figure 5 displays a correspondence between the discharged temperature and the condensed temperature with R744. It is assessed that the evaporating temperature of R513A has the compact to the condensed temperature and the discharged temperature of R744.

When the evaporating temperature of R513A goes down from 4.3 to 0.8°C, the condensation temperature of R744 reduces from 6.3 to 5.8°C and the discharge temperature of R744 also reduces from 66.5 to 62°C.

Figure 6 indicates a relationship between the condensed temperature of R744 in LTC and the cooling capacity when the evaporating temperature of R513A changes. When condensed temperature of R744 rises from 5.8 to 6.3°C, the evaporation temperature of R513A also goes up from 0.8 to 4.3°C, the cooling capacity goes down from 1.35 to 1.13 kW. Similarly, the COP of the CRS is indicated in Figure

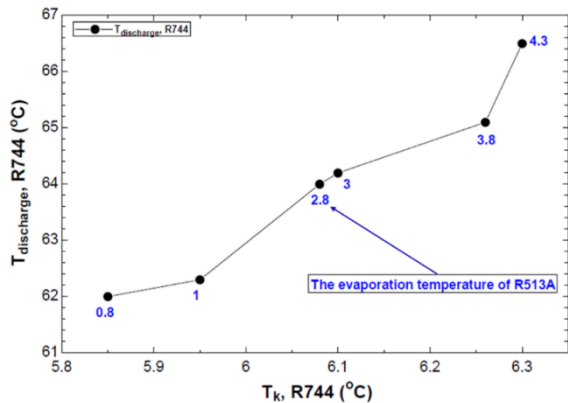


Fig. 5: The discharge temperature vs. the condensed temperature of R744

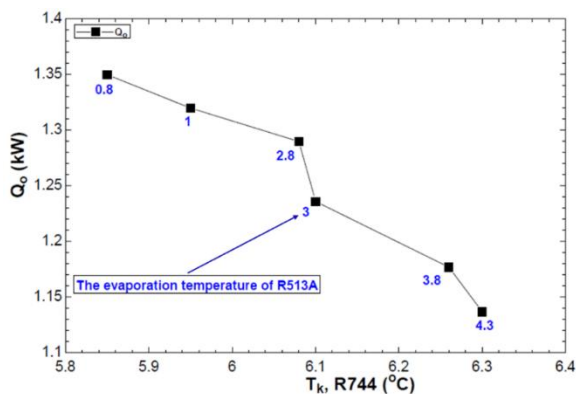


Fig. 6: The condensed temperature of R744 and the cooling capacity

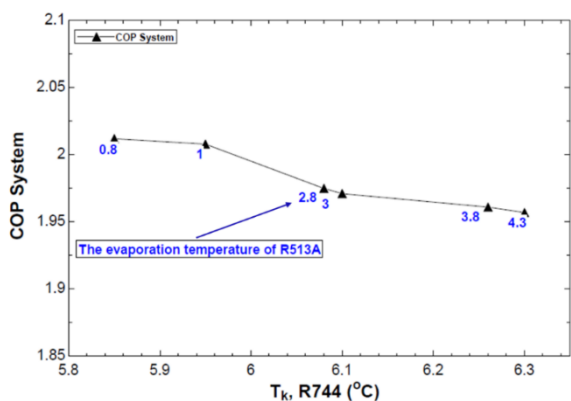


Fig. 7: The condensed temperature of R744 and COP

7. When the condensed temperature of R744 rises from 5.8 to 6.3°C, the COP declined from 2.01 to 1.96.

#### 4. Conclusion

This research has been conducted in an experiment with a cascade cold storage refrigeration system operating by R513A/R744 refrigerant pair. The R513A refrigerant was applied in HTC and R744 was applied in LTC.

The experimental results were gained under the surrounding temperature of 32°C. Also, in this study, the cold chamber temperature dropped from 32°C to -20°C over a period of 35 minutes. The thermodynamic behaviors of the CRS were shown in more specifically. R744 at LTC cycle has a condensed temperature of 5.8°C and an evaporating temperature of -25°C. The system cooling capacity is 1.35 kW and the COP is 2.0.

Furthermore, the theoretical calculations are compatible with the experimental results. It leads to distribute the supplement the researching data needed when studying stratified systems using R744 refrigerant in refrigeration field.

#### Acknowledgments

The assistance of this work by the project No. 11/2025/HĐ-QKHCN (sponsored by HCMC Department of Science and Technology, Vietnam) and the project No. T2026-O2NTĐ (sponsored by HCMC University of Technology and Engineering, Vietnam) is highly appreciated.

#### References

- 1) M. Purjam, K. Thu, and T. Miyazaki, "Thermodynamic Feasibility Evaluation of a novel low temperature ejector-based trans-critical R744 refrigeration cycle", *Evergreen*, 8 (1) 204–212 (2021). doi.org/10.5109/4372280.
- 2) G. Sachdeva, B. Sharma, P. Anuradha, and S. Verma, "Irreversibility analysis of an ejector refrigeration cycle by modified Gouy-Stodola formulation", *Evergreen*, 10 (1) 252–271 (2023). doi.org/10.5109/6781075.
- 3) T. Widiarti and H. Firdaus, "A Decade of Organic Rankine Cycle Research Trends and Evolution: A Bibliometric analysis", *Evergreen*, 11 (3) 2479–2503 (2024). doi.org/10.5109/7236890.
- 4) M.T. Kibria, Md.A. Islam, B.B. Saha, T. Nakagawa, and S. Mizuno, "Assessment of environmental impact for Air-Conditioning systems in Japan using HFC based refrigerants," *Evergreen*, 6 (3) 246–253 (2019). doi.org/10.5109/2349301.
- 5) N. Ashwni and N.A.F. Sherwani, "Assessment of the Impact of using Zeotropic Mixture on the Thermodynamic Performance of Organic Rankine

- Cycle Integrated Vapor Compression Refrigeration System”, *Evergreen*, 10 (2) 1094–1099 (2023). doi.org/10.5109/6793668.
- 6) C. Yang, N. Takata, T. Miyazaki, and K. Thu, “Low-GWP Refrigerant blends as Replacements of R410A for Domestic Heat Pumps”, *Evergreen*, 11 (2) 1435–1441 (2024), doi.org/10.5109/7183465.
  - 7) C. Amaris, K.M. Tsamos, and S.A. Tassou, “Analysis of an R744 typical booster configuration, an R744 parallel-compressor booster configuration and an R717/R744 cascade refrigeration system for retail food applications. Part 1: Thermodynamic analysis,” *Energy Procedia*, 161 259–267 (2019). doi.org/10.1016/j.egypro.2019.02.090.
  - 8) L. Nebot-Andrés, J. Catalán-Gil, D. Sánchez, D. Calleja-Anta, R. Cabello, R. Llopis, “Experimental determination of the optimum working conditions of a transcritical CO<sub>2</sub> refrigeration plant with integrated mechanical subcooling,” *International Journal of Refrigeration*, 113 266–275 (2020). doi.org/10.1016/j.ijrefrig.2020.02.012.
  - 9) M. Goodarzi, A. Gheibi, “Performance analysis of a modified trans-critical CO<sub>2</sub> refrigeration cycle,” *Applied Thermal Engineering*, 75 1118–1125 (2014). doi.org/10.1016/j.applthermaleng.2014.10.075.
  - 10) Y. Chen, H. Zou, J. Dong, H. Xu, C. Tian, D. Butrymowicz, “Experimental investigation on refrigeration performance of a CO<sub>2</sub> system with intermediate cooling for automobiles,” *Applied Thermal Engineering*, 174 115–267 (2020). doi.org/10.1016/j.applthermaleng.2020.115267.
  - 11) F.E. Manjili, M. Cheraghi, “Performance of a new two-stage transcritical CO<sub>2</sub> refrigeration cycle with two ejectors,” *Applied Thermal Engineering*, 156 402–409 (2019). doi.org/10.1016/j.applthermaleng.2019.03.083
  - 12) Z.-Y. Zhang, Y.-T. Ma, H.-L. Wang, M.-X. Li, “Theoretical evaluation on effect of internal heat exchanger in ejector expansion transcritical CO<sub>2</sub> refrigeration cycle,” *Applied Thermal Engineering*, 50 932–938 (2012). doi.org/10.1016/j.applthermaleng.2012.08.022
  - 13) Da Silva, E.P.B. Filho, A.H.P. Antunes, “Comparison of a R744 cascade refrigeration system with R404A and R22 conventional systems for supermarkets,” *Applied Thermal Engineering*, 41 30–35 (2011). doi.org/10.1016/j.applthermaleng.2011.12.019.
  - 14) Y. Zhang, Y. He, Y. Wang, X. Wu, M. Jia, Y. Gong, “Experimental investigation of the performance of an R1270/CO<sub>2</sub> cascade refrigerant system,” *International Journal of Refrigeration*, 114 175–180 (2020). doi.org/10.1016/j.ijrefrig.2020.02.017.
  - 15) H. Li, X. Gong, W. Xu, M. Li, C. Dang, “Effects of climate on the solar-powered R1234ze/CO<sub>2</sub> cascade cycle for space cooling,” *Renewable Energy*, 153 870–883 (2020). doi.org/10.1016/j.renene.2020.02.052
  - 16) R. Lizarte, M.E. Palacios-Lorenzo, J.D. Marcos, “Parametric study of a novel organic Rankine cycle combined with a cascade refrigeration cycle (ORC-CRS) using natural refrigerants,” *Applied Thermal Engineering*, 127 378–389 (2017). doi.org/10.1016/j.applthermaleng.2017.08.063
  - 17) D.A. Dokandari, A.S. Hagh, S.M.S. Mahmoudi, “Thermodynamic investigation and optimization of novel ejector-expansion CO<sub>2</sub>/NH<sub>3</sub> cascade refrigeration cycles (novel CO<sub>2</sub>/NH<sub>3</sub> cycle),” *International Journal of Refrigeration*, 46 26–36 (2014). doi.org/10.1016/j.ijrefrig.2014.07.012.
  - 18) K. Megdoui, N. Ejemni, E. Nahdi, A. Mhimid, L. Kairouani, “Thermodynamic analysis of a novel ejector expansion transcritical CO<sub>2</sub>/N<sub>2</sub>O cascade refrigeration (NEETCR) system for cooling applications at low temperatures,” *Energy*, 128 586–600 (2017). doi.org/10.1016/j.energy.2017.04.073.
  - 19) M. Sobieraj, M. Rosiński, “High phase-separation efficiency auto-cascade system working with a blend of carbon dioxide for low-temperature isothermal refrigeration,” *Applied Thermal Engineering*, 161 114–149 (2019). doi.org/10.1016/j.applthermaleng.2019.114149
  - 20) M. Aminyavari, B. Najafi, A. Shirazi, F. Rinaldi, “Exergetic, economic and environmental (3E) analyses, and multi-objective optimization of a CO<sub>2</sub>/NH<sub>3</sub> cascade refrigeration system,” *Applied Thermal Engineering*, 65 42–50 (2014). doi.org/10.1016/j.applthermaleng.2013.12.075.
  - 21) M. Ma, J. Yu, X. Wang, “Performance evaluation and optimal configuration analysis of a CO<sub>2</sub>/NH<sub>3</sub> cascade refrigeration system with falling film evaporator–condenser,” *Energy Conversion and Management*, 79 224–231 (2014). doi.org/10.1016/j.enconman.2013.12.021.
  - 22) K. Logesh, S. Baskar, M. Azeemudeen, B.P. Reddy, G.V.S.S. Jayanth, “Analysis of Cascade Vapour Refrigeration System with Various Refrigerants,” *Materials Today Proceedings*, 18 4659–4664 (2019). doi.org/10.1016/j.matpr.2019.07.450.
  - 23) N. Gautam, G. Kumar, S. Sahoo, “Performance improvement and comparisons of CO<sub>2</sub> based adsorption cooling system using modified cycles employing various adsorbents: A comprehensive study of subcritical and transcritical cycles,” *International Journal of Refrigeration*, 112 136–154(2019). doi.org/10.1016/j.ijrefrig.2019.12.008.
  - 24) Z. Sun, Q. Cui, Q. Wang, J. Ning, J. Guo, B. Dai, Y. Liu, Y. Xu, “Experimental study on CO<sub>2</sub>/R32 blends in a water-to-water heat pump system,” *Applied Thermal Engineering*, 162 114303 (2019).

- doi.org/10.1016/j.applthermaleng.2019.114303.
- 25) A. Messineo, "R744-R717 Cascade Refrigeration System: Performance Evaluation compared with a HFC Two-Stage System," *Energy Procedia*, 14 56–65 (2012). doi.org/10.1016/j.egypro.2011.12.896.
  - 26) A. Ghosh, A. Sharma, B. Varshney, N. Chirag, P.K. Kashyap, "A theoretical thermodynamic analysis of R1234YF/CO<sub>2</sub> cascade refrigeration system," in: *Lecture Notes in Mechanical Engineering*, 57–69 (2023). doi.org/10.1007/978-981-19-8517-1\_5.
  - 27) A. Ustaoglu, B. Kursuncu, M. Alptekin, M.S. Gok, "Performance optimization and parametric evaluation of the cascade vapor compression refrigeration cycle using Taguchi and ANOVA methods," *Applied Thermal Engineering*, 180 115816 (2020). doi.org/10.1016/j.applthermaleng.2020.115816.
  - 28) X. Liu, R. Fu, Z. Wang, L. Lin, Z. Sun, X. Li, "Thermodynamic analysis of transcritical CO<sub>2</sub> refrigeration cycle integrated with thermoelectric subcooler and ejector," *Energy Conversion and Management*, 188 354–365 (2019). doi.org/10.1016/j.enconman.2019.02.088.
  - 29) T.T. Dang, T.H. Nguyen, J.T. Teng, J.H. Lu, and B.C. Nguyen, "Numerical simulation of heat transfer phenomena in a microchannel evaporator for a transcritical CO<sub>2</sub> air conditioning system", *International Journal of Air-Conditioning and Refrigeration*, 32 (17)1-15 (2024), doi.org/10.1007/s44189-024-00062-y.
  - 30) T.T. Dang and H.T. Nguyen, "A Study on the Simulation and Experiment of Evaporative Condensers in an R744 Air Conditioning System," *Micromachines* 2023 (14) 1826 (2023), doi.org/10.3390/mi1410182.
  - 31) M. Yang, H. Zhang, Z. Meng, Y. Qin, "Experimental study on R1234yf/R134a mixture (R513A) as R134a replacement in a domestic refrigerator," *Applied Thermal Engineering*, 146 540–547 (2018). doi.org/10.1016/j.applthermaleng.2018.09.122.
  - 32) A. Mota-Babiloni, J.M. Belman-Flores, P. Makhnatch, J. Navarro-Esbrí, J.M. Barroso-Maldonado, "Experimental exergy analysis of R513A to replace R134a in a small capacity refrigeration system," *Energy*, 162 99–110 (2018). doi.org/10.1016/j.energy.2018.08.028.
  - 33) A. Mota-Babiloni, P. Makhnatch, R. Khodabandeh, J. Navarro-Esbrí, "Experimental assessment of R134a and its lower GWP alternative R513A," *International Journal of Refrigeration*, 74 682–688 (2016). doi.org/10.1016/j.ijrefrig.2016.11.021.
  - 34) A. Mota-Babiloni, J. Navarro-Esbrí, V. Pascual-Miralles, Á. Barragán-Cervera, A. Maiorino, "Experimental influence of an internal heat exchanger (IHX) using R513A and R134a in a vapor compression system," *Applied Thermal Engineering*, 147 482–491 (2018). doi.org/10.1016/j.applthermaleng.2018.10.092
  - 35) J. Sun, W. Li, B. Cui, "Energy and exergy analyses of R513a as a R134a drop-in replacement in a vapor compression refrigeration system," *International Journal of Refrigeration*, 112 348–356 (2019). doi.org/10.1016/j.ijrefrig.2019.12.014.